PERGAMON

Deep-Sea Research II 49 (2002) 693–706

DEEP-SEA RESEARCH
PART II

www.elsevier.com/locate/dsr2

Physical gradients and spatial variability of the size structure and composition of phytoplankton in the Gerlache Strait (Antarctica)

Jaime Rodríguez*, Francisco Jiménez-Gómez, José M. Blanco, Félix L. Figueroa

Departamento de Ecología y Geología, Facultad de Ciencias, Universidad de Málaga, Campus de Teatinos, 29071-Málaga, Spain

Received 14 April 1998; received in revised form 9 June 1999; accepted 14 June 2001

Abstract

The patterns of variability of the size structure and functional composition of phytoplankton are closely linked to physical gradients in the coastal waters of the Gerlache Strait (Antarctic Peninsula). Different stratified conditions are found at both extremes of the Strait, separated by a large, rather vertically homogeneous body of water. In the SW extreme close to Bellingshausen Sea, a cold upper layer representative of ice melting influence is dominated by microplankton (20–100 μm ESD) biomass, mainly composed of colonies or aggregates of *Phaeocystis* in bloom stage. In the NE extreme close to Bransfield Strait, a warm surface layer has a 10–20 μm nano planktonic community dominated by *Cryptomonas* and a diverse assemblage of ultraplanktonic (2–10 μm) flagellates. In this area, microplankton larger than 40 μm ESD is almost absent at the sample volume studied. Also in terms of biomass, mixed central waters are dominated by microplankton, particularly large diatoms. Our results show that diatoms and microplankton are the dominant categories under turbulent conditions, with typical flagellate blooms (*Phaeocystis* and *Cryptomonas*) under particularly stratified conditions. In terms of numerical abundance, however, ultraplanktonic flagellates usually dominate the community, giving a bell shaped size-abundance spectra in all the regions and supporting previous suggestions of flagellate dominance even under mixed-layer conditions. © 2001 Published by Elsevier Science Ltd.

1. Introduction

The open waters of the Southern Ocean are a "high nutrient–low chlorophyll" region (Chisholm and Morel, 1991; Tréguer and Jacques, 1992), a feature that has stimulated discussion about which factors control phytoplankton growth and biomass accumulation in Antarctic waters (Cullen, 1991). However, phytoplankton distribution is patchy at different spatial and temporal scales (Schloss and Estrada, 1994), and different hydrodynamic singularities (sensu Legendre and Le Fèvre, 1989) like fronts, marginal ice-melting zones or mesoscale eddies may represent loci of increased growth rate and biomass accumulation. This is particularly relevant in different areas of the Antarctic coastal waters, where blooms of diatoms, the prymnesiophyceae *Phaeocystis* or the cryptophyte *Cryptomonas* are conspicuous phenomena.

The study of bloom dynamics has attracted much attention (see Heywood and Whitaker,

*Corresponding author. Tel.: +34-952-1311850; fax: +34-952-1312000.

E-mail address: jaime_rodri@uma.es (J. Rodríguez).

0967-0645/01/$ - see front matter © 2001 Published by Elsevier Science Ltd.
PII: S0967-0645(01)00119-9

1984) and generated discussion about the factors that determine the dominance of diatoms or flagellates (Estrada and Delgado, 1990; Smetacek et al., 1990; Bianchi et al., 1992; Lancelot et al., 1993; Schloss and Estrada, 1994; Socal et al., 1997). As Schloss and Estrada (1994) point out, the question of the dominance of diatoms versus flagellates is not only of theoretical interest, since it represents the dominance of large versus small size cells. The implications of the relative dominance of different taxonomical groups on the size structure of the community have to be taken into account in the analysis of the fate of phytoplankton production, its flow through grazing or microbial food webs, the importance of sinking and export production and, consequently, the evaluation of carbon fluxes through the water column. Because of the clear links between physical forcing, biological productivity and planktonic food web structure, the study of the relationships between size structure of the phytoplankton community and hydrodynamical features like oligotrophic gyres, upwelling and fronts is an active area of research in many ocean regions (Chisholm, 1992; Li, 1994; Rodríguez and Li, 1994; Rodríguez et al., 1998) but remains largely unexplored or contradictory in Antarctic waters.

The size structure of phytoplankton is usually approached through fractionation of chlorophyll, ATP or similar aggregate biomass descriptors (see, for example, Bienfang and Szyper, 1981; Laubscher et al., 1993; Rodriguez and Guerrero, 1994; Varela et al., 2002). The information obtained through these methods in Antarctic waters is contradictory or nonconclusive. The fractionation approach was followed by Helbling et al. (1991) to described a shift from a nanoplankton-dominated community to one dominated by microplankton after iron addition. On the other hand, Holm-Hansen and Mitchell (1991) and Karl et al. (1991) described a shift from microplankton to nanoplankton dominance as the phytoplankton bloom matures and declines in the coastal waters of the Antarctic Peninsula. A different pattern was found by Savidge et al. (1995) in the Bellingshausen Sea, where microplankton seems to dominate at different values of total phytoplankton biomass.

In this paper, an analysis of the size structure and the functional composition of the Antarctic phytoplankton is presented, through a combination of flow cytometry and image analysis techniques that permit the characterisation of the complete size-abundance spectrum of photoautotrophic cells. As a general pattern, it will be shown that Antarctic size-abundance spectra are dominated by ultraplanktonic flagellates. At the regional scale, the study will show how changes in water column structure can be associated to shifts in the size structure and composition of the phytoplankton community.

2. Methods

2.1. The area of study

The general description of FRUELA cruise logistics can be found in Anadón and Estrada (2002). Data in this paper derive from two SW–NE transects carried out within the coastal and sheltered waters of the Gerlache Strait (Fig. 1) during the first Fruela cruise. The first transect,

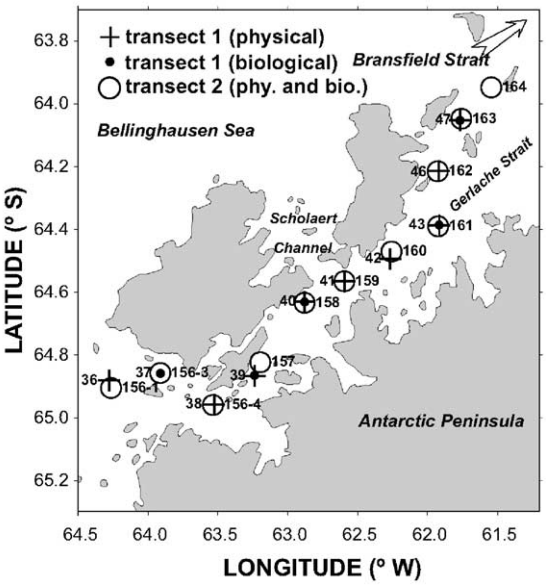

Fig. 1. Area of study and sampling stations in the first and second transects along the Gerlache Strait

covering a total of nine stations, was completed in two days (December, 10–11, 1995). The second transect, covering a total of eleven stations was completed in four days (December, 20–23). García et al. (2002) have demonstrated that the overall physical structure of the Gerlache region remained qualitatively constant during the two Fruela crusises (December 95 and January 96), thus reducing the problem of the lack of synopticity of the observations within any of our two surveys.

2.2. Sampling

Water column profiles of temperature, salinity and fluorescence were obtained with a CTD GO MKIIIC WOCE Probe provided with extra oxygen, fluorescence and light-transmission sensors. A profiling Sea Tech transmissometer (25-cm pathlength) was used to determine the percentage of light transmission of the water at each depth (Figueroa, 2002). The beam attenuation coefficient (c) expressed in m^{-1}, which is a good estimator of the concentration of particulate material, was calculated according to the equation:

$$c = (\mathrm{Ln}\, T)/z$$

T being transmission and z the path length of the transmissometer (0.25 m).

Water samples were taken from the rosette bottles at different depths within the upper 100 m of the water column for the analysis of the size structure and composition of the phytoplankton community. A volume between 5 and 10 ml was dedicated to the on board flow cytometry analysis of cell populations. Another 100 ml were preserved with lugol for the later microscopy analysis at the laboratory of Ecology.

2.3. Flow cytometry

Water samples were filtered through 80-μm mesh and then directly analysed with a FacScan (Becton Dickinson) flow cytometer. The following acquisition parameter settings were defined: FSC = E00; SSC = 271; FL1 = 450; FL2 = 450; FL3 = 300 with a logarithmic amplification for each signal and a threshold for chlorophyll fluorescence (FL3 = 001). Sample volume was deduced from the time of analysis (300 s) and the selected flow rate (*"high"* setting = 80 μl min^{-1}). Flow rate was calibrated at the beginning and at the end of the sampling period. Data were acquired in list mode and processed with Lysis II®, CellQuest® and Attractor® software.

Through flow cytometry, we discriminated three size groups of eukaryotic cells that roughly correspond to picoplankton (up to 2 μm ESD, equivalent sphaerical diameter), ultraplankton (or "small nanoplankton" cells between 2 and 10 μm ESD), and "large nanoplankton" cells between 10 and 20 μm (Fig. 2). A fourth and highly characteristic population within the large-nanoplankton size category is that formed by the flagellate *Cryptomonas*, easily separated from the common size compartment thanks to the orange fluorescence of phycoerythrin. No relevant signals of the presence of cyanobacteria or other phototrophic prokaryotes were detected.

2.4. Image analysis

At the laboratory, after sedimentation of the lugol's preserved samples, cells and colonies were counted and measured at 100 × and 200 × magnifications in a Nikon TM2 inverted microscope connected to a VIDS-IV (Analytical Measuring Systems) videointeractive image analysis system.

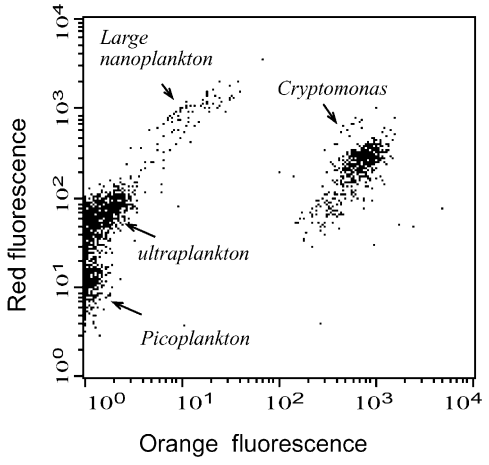

Fig. 2. Flow cytometric plot of the size-functional groups identified.

Process protocols can be found in Echevarría and Rodríguez (1994) and Ruiz et al. (1996). The size range analysed through microscopy and image analysis was dominated by diatoms, with a minor presence of dinoflagellates and localised abundance of *Phaeocystis* aggregates. The current sample volume taken during this study (100 ml), permitted the correct quantification of cell sizes up to approximately $10^6\,m^3$ (some 100 μm ESD). In fact, we shall see that, under some environmental conditions, cells larger than 40 μm were so scarce that they were not adequately represented in the 100 ml sample volume.

2.5. Size-abundance spectra

The transformation of the forward light scattering signals of the flow cytometer to cell volume was carried out through a calibration curve taken from Jimenez-Gomez (1995, unpublished results). Light scattering and image-analysis cell volume were measured for the following cell cultures: *Synechococcus* sp. (~1 μm), *Nannochloris atomus* (~2–4 μm), *Nannochloropsis gaditana* (~2–5 μm), *Isochrysis galbana* (~3–5 μm), *Phaeodactilum tricornutum* (~3–6 μm) and *Tetraselmis chui* (~8–11 μm). The flow cytometry signatures of these cells and the resulting calibration are shown in Fig. 3.

The coupling of flow cytometry and image analysis analytical subranges generates a "size (log_2 volume scale)—abundance" spectrum of phytoplankton that adequately covers the ensemble of the autotrophic community (Fig. 4). The considered phytoplankton size range extends from picoplanktonic cells larger than 0.5 μm up to a maximum cell size around 100 μm ESD. The analysis through flow cytometry extends from the smallest eukaryotic picoflagellates up to the upper limit of nanoplankton (20 μm). Image analysis covers the remaining size range up to largest microplanktonic diatoms and aggregates. Both methodologies overlap between 10 and 20 μm, the "large nanoplankton" size category (Fig. 4). In the size range where both methodologies overlap and produce independent abundance measurements (the size range occupied by the flagellate *Cryptomonas*), we assumed that the flow cytometry analysis of fresh samples was a more reliable method of abundance estimation than the later, microscopy study of preserved samples.

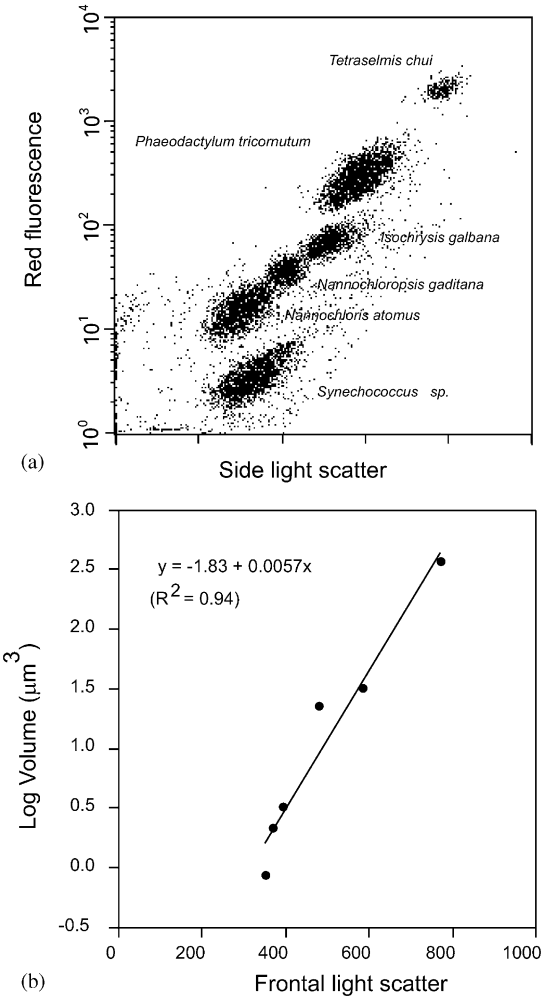

Fig. 3. (a) Flow cytometric pattern of the six cultured species employed in the calibration of the optical signals. (b) Relationship between frontal light scatter channel and cell volume for the phytoplankton cultures.

From the size-abundance spectrum, biovolume ($\mu m^3\,ml^{-1}$) for a particular size-compartment or functional group can be obtained as the area below the size spectrum, computed as

$$B = \sum V_i(n_i + n_{i+1})/2,$$

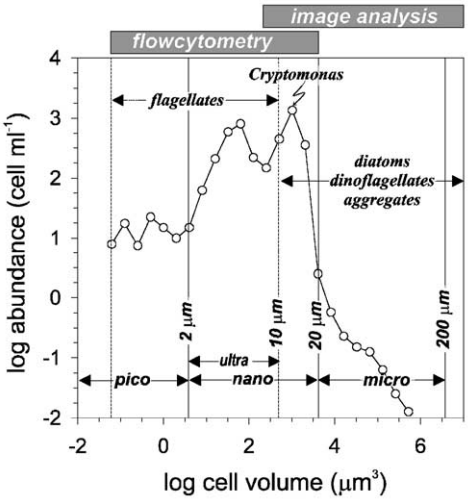

Fig. 4. Typical size-abundance spectrum from the combination of flow cytometry and image analysis.

where n_i is the number of cells in the size class (V_i, V_{i+1}), which is identical to $(V_i, 2V_i)$ because of its amplitude V_i (see Blanco et al., 1994).

3. Results

3.1. Basic physical features

The general water mass structure of the Gerlache Strait is described by Garcia et al. (2002). The basic features of the upper (100 m) water column, where physical properties show the impact of local sources of variability and, at the same time, are expected to have a clear effect on phytoplankton spatial distributions. According to García et al. (op. cit), the 100 m upper layer of the western Gerlache Strait (open to the Bellingshausen Sea) is occupied by Antartic Surface Water (AASW). There is a sharp transition from AASW to Transitional Waters with Bellingshausen influence (TBW) at approximately the position of station 39, Figure 5a shows that there is a cold and diluted upper layer ($\sim$40 m thick) within AASW that probably reflects the effect of ice melting in the nearby Bellingshausen Sea. The stratification characteristics were accentuated during the second survey 10 days later (Fig. 5b), when the water column showed a narrow surface layer of colder and more diluted water than earlier. The temperature profile showed the opposite tendency at the eastern part of the Strait, open to Bransfield Strait. The TBW water column was also stratified but, in this case, due to the presence of an upper layer, $\sim$40 m thick, of warm and diluted water (Fig. 5a). The stratification was also accentuated during the second survey ten days later (Fig. 5b) and, at the same time, a sharp front established between the stratified water column and the central Gerlache region. Here, the distribution of physical properties suggests mixing within the TBW water mass.

In both surveys (Fig. 5a and b), a relative maximum in situ fluorescence values was found in the vertically mixed region, with a $2\times$ increase between the first to the second survey. Vertical profiles of the beam attenuation coefficient (c) were rather homogeneous in the mixed, central region, with values between 1 and 1.5 m^{-1} at surface, and decreasing slightly with depth (Fig. 6). Similar values around 1.5 characterised a layer 25 m thick within the cold and diluted surface waters, dropping quickly to $<1\,m^{-1}$, and then decreasing very slowly with depth. The most striking profiles were found in the NE stratified region. During the first transect, the attenuation coefficient showed values close to 3 m^{-1} in the first 10 m of the upper warm layer (Fig. 6), and a sharp transition (5 m width) to values below 1 m^{-1}, which extended up to 40 m, the maximum depth where measurements were taken. During the second survey, there was a peak at 10 m depth where c reached a value of 4 m^{-1}. Values were around 1 m^{-1} at surface and decreased exponentially from the peak to 50 m depth ($c<1\,m^{-1}$).

3.2. Spatial distribution of pico-, ultra- and nanoplankton

In terms of numerical abundance, phytoplankton analysed through flow cytometry was dominated by ultraplankton. These cells reached abundances exceeding 3×10^3 ml^{-1} in the upper layer of the stratified water column at both ends of the Gerlache Strait (Fig. 7). This suggests that stability due to low surface salinity is the main

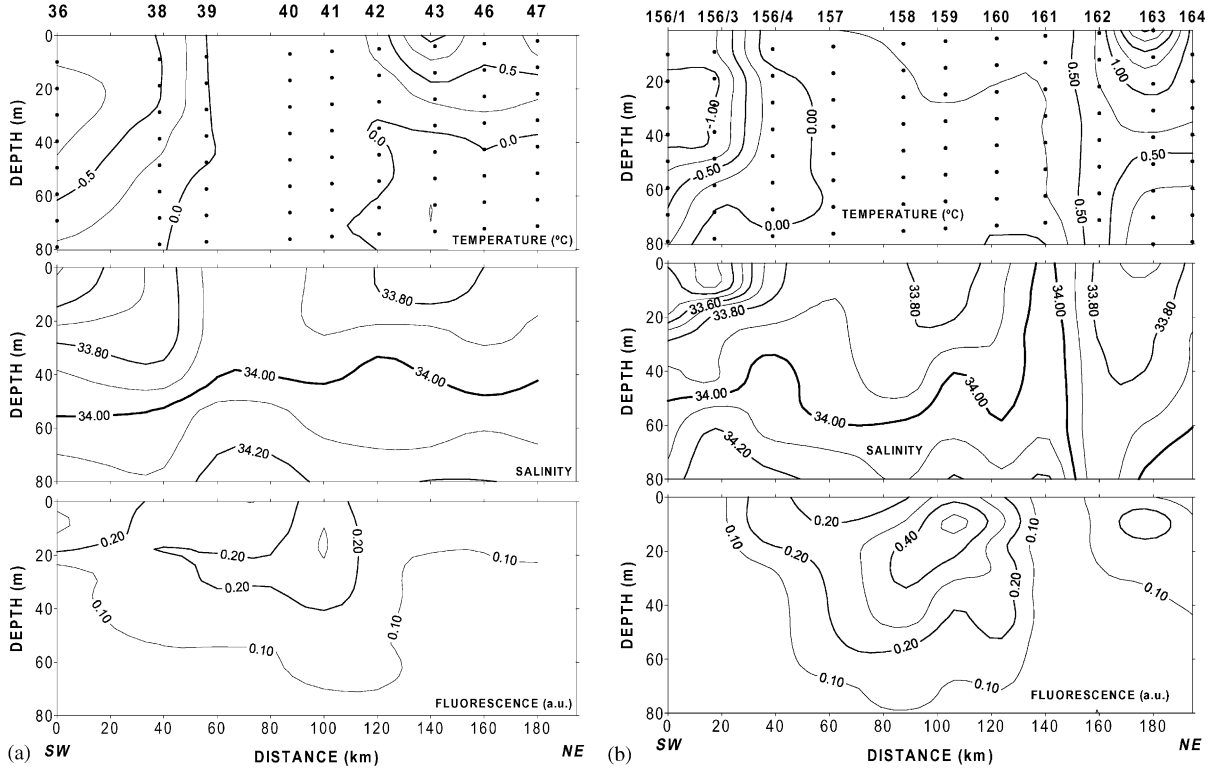

Fig. 5. Temperature (upper), salinity (middle) and fluorescence (bottom) distribution along the first (a) and second (b) transects.

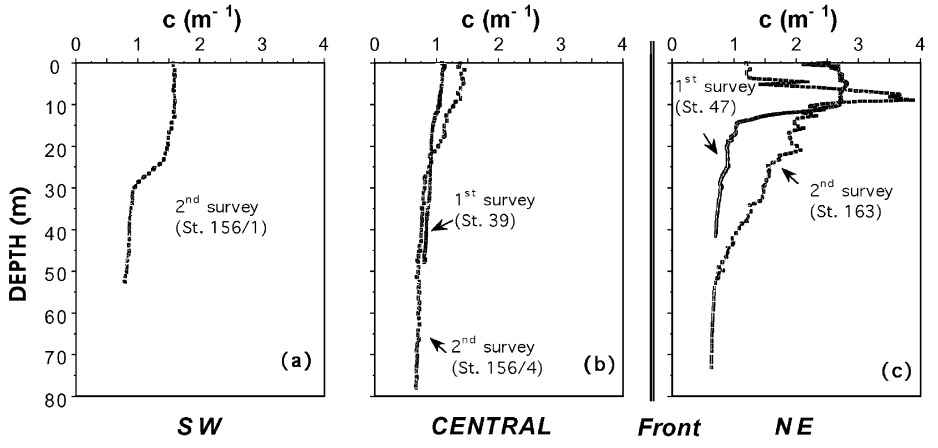

Fig. 6. Vertical profiles of the beam attenuation coefficient at representative stations of the first and second surveys.

physical feature favouring the observed distribution, since surface temperature shows an opposite gradient in both cases (Fig. 5). An interesting pattern was observed during the second survey after the development of the physical front, where, in correspondence with the strong vertical

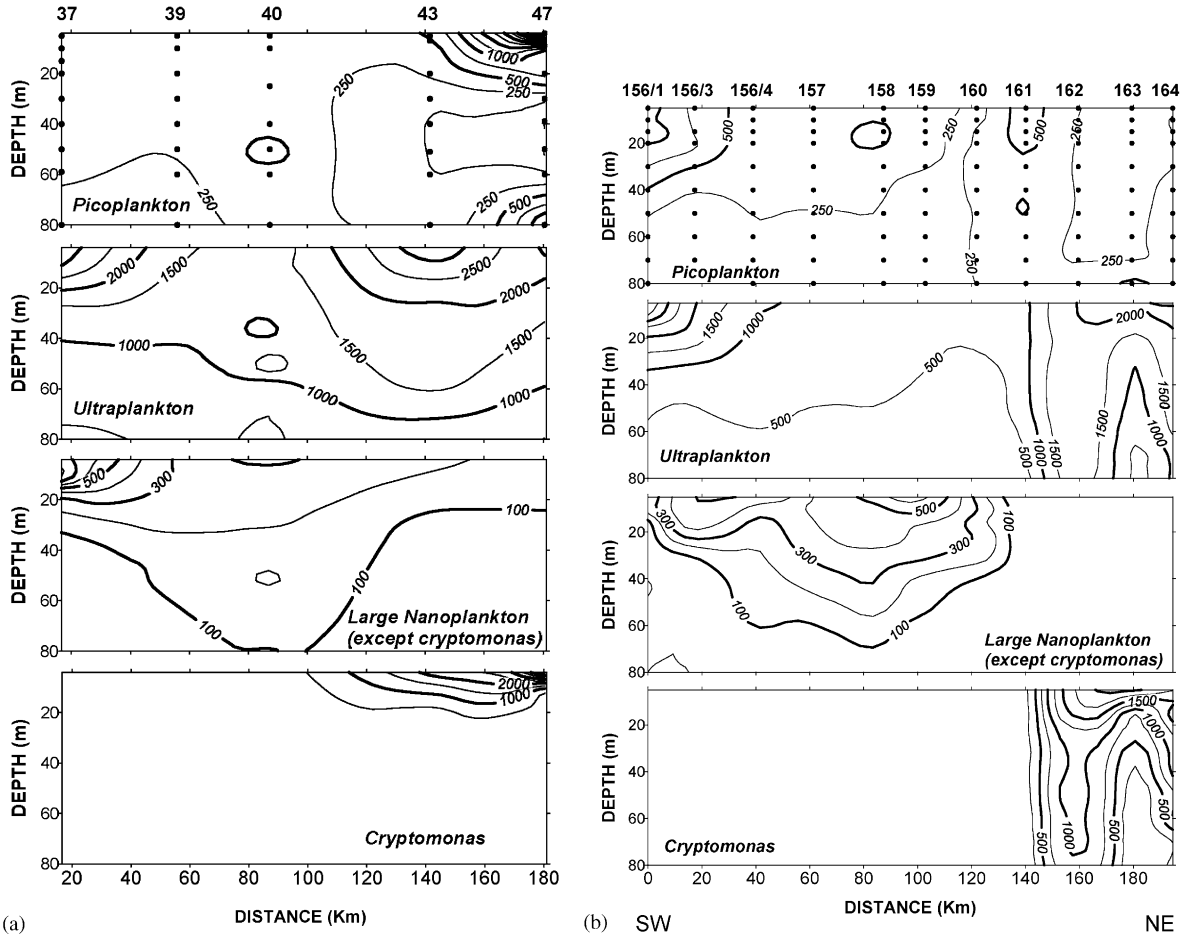

Fig. 7. Size-functional groups pico-, ultra- and large nanoplankton and *Cryptomonas* distribution in the water column along the first (a) and second (b) transects. See Fig. 4 for the corresponding size ranges.

mixing indicated by temperature and salinity, ultraplanktonic flagellate distribution was vertically homogeneous along the sampled water column (Fig. 7b).

The large-nanoplankton size category comprised two distinct components: an heterogeneous, diatom-dominated and a characteristic population of the flagellate *Cryptomonas*. The first component reached abundance only slightly greater than 500 cells ml^{-1}. Their initial focus was linked to the cold and diluted surface waters close to Bellingshausen (Fig. 7a), and later they extended to occupy all the middle Gerlache (Fig. 7b). The *Cryptomonas* population was initially limited to the warm and diluted surface layer close to Bransfield Strait (Fig. 7a), with densities higher than 6×10^3 cells ml^{-1}. Once the front was developed, *Cryptomonas* cells followed the same trend as ultraplaktonic flagellates and the physical descriptors, showing highly homogeneous vertical distribution in the water column (Fig. 7b). Although still high, the abundance of *Cryptomonas* in the northeast surface patch decreased to half the concentration observed ten days earlier.

As Fig. 7 shows, picoplanktonic cells were initially abundant in the same patch of warm

and diluted water than *Cryptomonas*, but they dispersed to low concentrations in the entire region at the moment of the second survey. The bulk of the compartment was composed of eukaryotic picoflagellates. No cyanobacteria cells were detected.

3.3. Size structure of phytoplankton

As a general trend, in terms of numerical abundance size distributions were dominated by ultraplanktonic (2–10 μm ESD) flagellates, with maximum densities in the size classes around $10^2\,\mu m^3$ ($\sim 6\,\mu m$ ESD). This feature, together with the low abundance of cells within the picoplankton size range, gives a bell-shaped structure to the Antarctic size-abundance spectra (Fig. 8). In all cases, cell abundance decreased in an almost continuous mode from the modal size classes both towards picoplankton and microplankton. Variability of the basic structure affects to (i) the sharpness of the ultraflagellate maximum, (ii) the length of the microplankton size range, and (iii) the presence of a second peak in the large-nanoplankton size classes (around $10^3\,\mu m^3$, $\sim 12\,\mu m$ ESD) (Fig. 8c). This variability was clearly related to the physical environment as will be shown in the following paragraphs.

Fig. 8 shows the differences between size spectra corresponding to the surface layer in the three physical environments that characterised the Gerlache Strait during the period of study. The most simple and regular spectra were found in the central, vertically mixed region. There was no sharp maximum there, abundance decreased smoothly towards both sides and the microplankton size range was adequately represented in the spectrum of abundances. Moreover, the size spectrum remained rather invariant between surveys. The most striking departure from this structure was found in the warm surface layer of NE stratified region (Fig. 8c), where we found the three elements of variability. Firstly, the ultraflagellage maximum was sharper than it was in other waters because of the higher cell densities of the modal size classes and the lower densities of the rest of ultraplankton and picoplankton size classes. Whereas modal cell abundance was similar during both surveys, abundance of the remaining ultra- and picoplankton size classes clearly decreased from the first to the second survey (Fig. 8c). Secondly, there was a second flagellate peak within the large-nanoplankton size compartment, clearly identified through flow cytometry and microscopy as a characteristic *Cryptomonas* population. Thirdly, no detectable cells or aggregates larger than $3 \times 10^4\,\mu m^3$ (some 40 μm ESD) were detected. The resulting spectrum showed an abrupt slope from the *Cryptomonas* maximum towards the low-density microplanktonic size

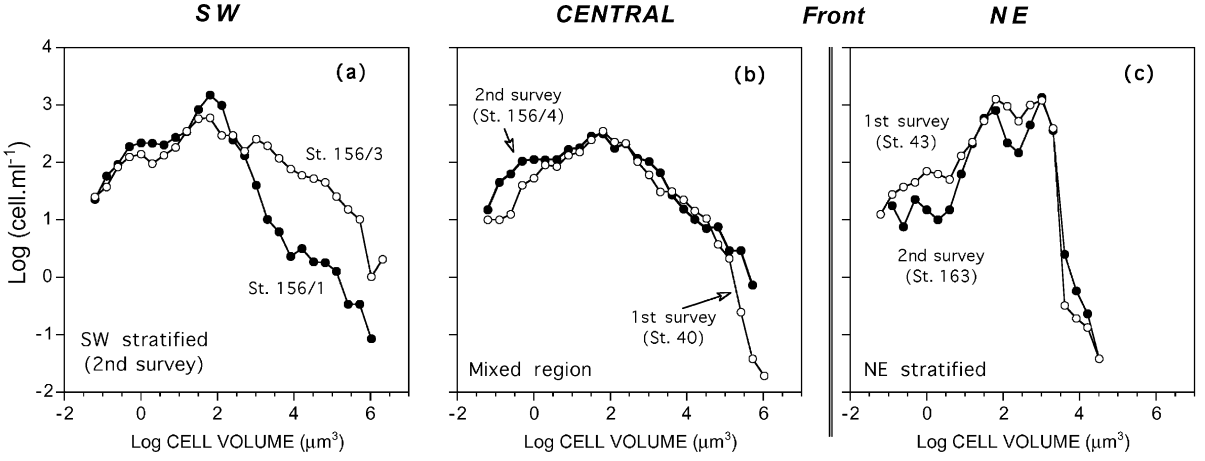

Fig. 8. Phytoplankton size-abundance spectra corresponding to the three physical environments which characterised the Gerlache during the period of study at 5 m depth.

classes with no relevant changes during the time interval between surveys.

The cold surface layer of the southwest stratified region exhibited a clear small-scale spatial heterogeneity. The two spectra in Fig. 8a obtained in the second survey (we could not obtain complete size distributions during the first survey) were separated by less than 20 km (Fig. 1). The spectrum in the station nearest to Bellingshausen Sea (156/1) presented a sharp ultraflagellate maximum similar to that found in the warm surface layer of the stratified northeast region. The differences with this are that (i) there were no a second, large-nanoflagellate (*Cryptomonas*) peak, and (ii) the complete microplankton size range was well represented in terms of abundance. In fact, it is within the microplankton size range where a net change occurs between the two sampling points (Fig. 8a), due to the presence of a bloom of diverse diatoms and *Phaeocystis* aggregates.

Size spectra presented different patterns of vertical variability in the three regions previously identified. In the vertically more homogeneous, central region (st. 156/4, Fig. 9b) size spectra maintained their shape although abundance values decreased continuously between 0 and 50 m depth. In the stratified water column of southwest region (156/1, Fig. 9a) most of the pico- and ultraplankton size range remains almost constant with depth. Densities associated to the ultraflagellate peak, large nanoplankton and microplankton size classes decreased with depth, with the result of a modal displacement to the left in the size range (Fig. 9a). In the case of the northeast stratified water column (st. 163, Fig. 9c), the ultraflagellate peak maintained its sharpness between 0 and 50 m depth. The most conspicuous vertical change here was the continuously decreasing and final disappearance of the large nanoflagellate (*Cryptomonas*) peak, illustrating the tendency of this population to accumulate at surface in the stratified water column.

In agreement with previous arguments, the size distribution of biovolume ($\mu m^3\,ml^{-1}$) exhibited a sharp horizontal change imposed by the presence of the front between the central and northeast regions, whereas the basic pattern of the distribution persisted through the time between surveys (Fig. 10). In the central mixed water column, biomass was dominated by microplankton ($>20\,\mu m$), followed (one order of magnitude lower) by similar amounts of ultraplankton (2–10 μm) and large nanoplankton (10–20 μm). Picoplankton ($<2\,\mu m$) biomass was almost three orders of magnitude lower than that of microplankton (Fig. 10b). In the frontal and stratified water column of the eastern region (Fig. 10c), biomass was clearly dominated by nanoplankton,

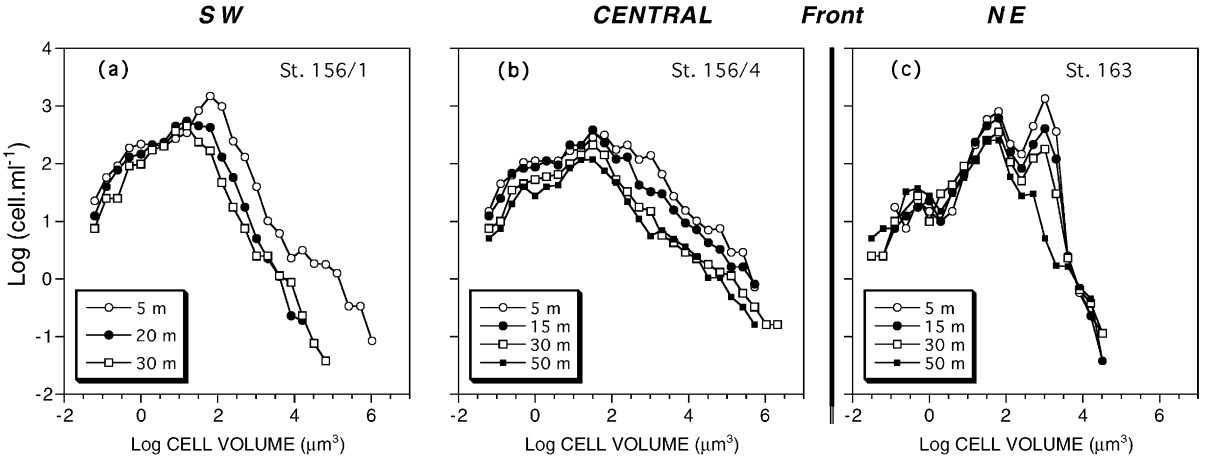

Fig. 9. Vertical variability of the phytoplankton size-abundance spectrum during the second survey corresponding to the three physical environments.

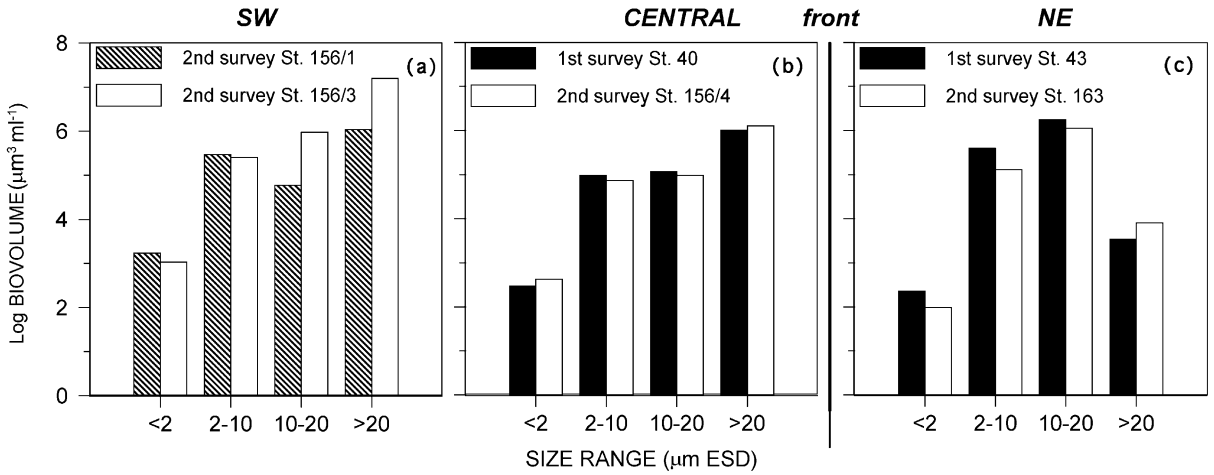

Fig. 10. Size distribution of biovolume corresponding to the categories defined in Fig. 4 in the same sites than Figs. 8 and 9.

particularly by the large-nanoplankton category, whose biomass increased one order of magnitude in relation to the western side of the front. Microplankton biomass decreased more than two orders of magnitude, and picoplankton maintained similar low biomass values relative to the central region. The situation found in the stratified southwest water column (Fig. 10a) was rather unique. Where the presence of aggregates characterises the planktonic community (st. 156/3) biovolume increased from picoplankton to microplankton compartments, the later reaching the highest values observed. In the other case (st. 156/1), microplankton and ultraplankton dominated over picoplankton and large nanoplankton.

4. Discussion

The Gerlache Strait appears as a highly heterogeneous region where physical gradients and discontinuities determine phytoplankton spatial variability at many levels (size-spectrum shape, size-distribution of biomass, taxonomic or functional group, coexistence or segregation, etc.). The ecosystem can be physically divided into two stratified regions at both extremes of the Strait separated by a more or less vertically mixed region. A sharp front is established between the central mixed region and the NE stratified area, where the temperature profile suggests the advective origin of a surface layer of warm and diluted water. On the other extreme (SW) the proximity of packed ice in the Bellingshausen coastal zone determines an inverse stratification, with cold but diluted water in the upper layer. The transition between this zone and the mixed water column is not as sharp as in the NE boundary, but biological communities also appear to vary along the physical gradient.

An adequate light availability associated to vertical stability seem to favour phytoplankton blooms in Antarctic waters (El-Sayed, 1971; Smith and Nelson, 1985; Holm-Hansen et al., 1989). Stabilisation in the SW Gerlache appears to be the result of ice melting in the proximity of Bellingshausen Sea (see Fig. 5b). Less than 20 km from the packed ice, phytoplankton community changes from an ultraflagellate-dominated assemblage (more than 10^6 cells l^{-1}), with abundant diatoms and some *Phaeocystis* colonies, to the core of a mixed bloom where microplanktonic diatoms and *Phaeocystis* colonies reached abundance in excess $10^5 l^{-1}$. *Phaeocystis* has been cited as a typical bloom forming species in Antarctic waters, often in connection with ice (Estrada and Delgado, 1990 and references therein). In terms of individual cell abundance, the figure for *Phaeocystis* is much

higher because, in addition to those included within the colony matrix, free cells in the size range of ultraplanktonic flagellates surely contribute to the peak shown by the size-abundance spectrum in this area (Fig. 8a). Stoecker et al. (1995) describe a spring *Phaeocystis*–diatom bloom in the edge of the annual sea ice in McMurdo Sound with individual cell densities higher than $10^6 l^{-1}$ and diatom density around one order of magnitude lower. From the size structure of aggregates in our sample volume and a relation between colony size and cells per colony (data not shown), we can estimate a *Phaeocystis* density in the order of 10^8 colonial cells l^{-1}. Consequently, the total cell abundance including the free-cells component is much higher than peak values reported by Putt et al. (1994) and Stoecker et al. (1995) during the bloom sequence in McMurdo Sound. Covariance between *Phaeocystis* and diatoms is controversial (Palmisano et al., 1986; Fryxell and Kendrick, 1988; Estrada and Delgado, 1990), and some authors (Davidson and Marchant, 1992) have suggested an inhibitory effect of *Phaeocystis* on other autotrophs. Such an effect is not supported by the shape, the length of the size range or the diverse composition of the size-abundance spectrum of the phytoplankton community in our observations (Fig. 8a).

At the other extreme of the Strait, the warm and diluted upper layer of the water column encloses a dense population of the nanoflagellate *Cryptomonas*, with surface concentrations in the order of $2–4 \times 10^6$ cells l^{-1}. Abundance of cryptomonads has been reported by different authors in Antarctic waters (see Schloss and Estrada, 1994 and references therein). They are frequently associated with low-salinity, highly stable water layers where they can maintain by active swimming, or to the confluence of different water masses with high phytoplankton biomass values (Schloss and Estrada, 1994; Mura et al., 1995). Our size spectrum distributions (Figs. 8c and 9c) indicate that *Cryptomonas* dominance runs parallel to the scarcity of microplankton. The phototrophic community in the surface layer is then characterised by the nanoplankton size compartment that we have identified as the summation of ultraplankton (2–10 μm) and large-nanoplankton (10–20 μm). The bloom of *Cryptomonas* is the cause of the very high attenuation values found in this area (Fig. 6c). During the first cruise a very narrow layer with c values close to $4\,m^{-1}$ was found at 10 m depth. During the second survey, values close to $3\,m^{-1}$ were characteristic of a surface layer 10 m think. These values are even higher than those found by Mitchell and Holm-Hansen (1991) in the same area and also under bloom conditions and illustrate that short-term variability of phytoplankton patchiness may have a clear effect on the optical properties of the water column.

The presence of *Cryptomonas* also has been related to a successional change occurring after a diatom bloom (Moline and Prézelin, 1996), agreeing with the basic scheme proposed by Margalef (1978) where the succession from diatoms to flagellates follows the transition from mixed to stratified waters. The mixture of hydrographical conditions at the regional and local scales in Antarctic waters makes it very difficult to strictly link these biological changes to a successional process without the necessary time series of observations. Most of the times, local or regional transport and advection of water masses has to be considered as an alternative a hypothesis (Bianchi et al., 1992; Schloss and Estrada, 1994). In fact, observations during the second survey suggests the importance of vertical transport at the front as a mechanism of reducing the surface accumulation of *Cryptomonas*, which maintain similar concentrations over the whole water column. Consequently, a correct interpretation probably should combine transport within a particular water mass and active growth under locally sheltered and stable conditions of the water column.

Flow cytometry measurements in the vertically mixed central area of the Gerlache show the accumulation of a low-density population of large-nanoplanktonic cells (*Cryptomonas* not included) whereas ultraplanktonic flagellates concentrate at the stratified extremes of the region. On the other hand, microscopy and image analysis of preserved samples from this mixed central region reveals the importance of the microplanktonic (mainly diatoms) components, which extends the size range up to $\sim 10^6\,\mu m^3$ cell

volume. Size integration of spectra (Fig. 10b) shows that here biomass is dominated by microplankton, which is coherent with proposals by Margalef (1978) and observations of the size distribution of biomass in other oceanic regions (Rodríguez et al., 1998). The low-population density that characterises this area, particularly during the first survey, seems to slow the low and vertically homogeneous attenuation values in all the water column (Fig. 6b), although the values are slightly higher than those found by Mitchell and Holm-Hansen (1991) in open Antarctic waters. The increase of the concentration of phytoplankton observed during the second survey of the area is the cause of the corresponding increase of the beam attenuation coefficient value up to $1.5\,m^{-1}$ in the first 20 m of the water column. The complete profile can still be considered as rather homogeneous when compared with profiles of the stratified water bodies at both ends of the Strait.

In terms of cell density, the phytoplankton community in these Antarctic waters was dominated by flagellates. In fact, Smetacek et al. (1990) suggested that diatom blooms are sporadic events that take place in a flagellate dominated community. In this same line, Kopczynska (1992) described a low-density, flagellate-dominated community under vertical mixing conditions, in apparent contradiction with the general association between "large diatoms—mixing" and "small flagellates—stratification". It is clear, as Schloss and Estrada (1994) point out, that the term "flagellate" is ambiguous and encompasses an enormous diversity of species and sizes. Our size-abundance spectra show that, in terms of density or numbers, ultraplanktonic flagellates represent the dominant component of the phytoplanktonic community in these Antarctic coastal waters, and even can dominate biomass under stratification conditions. However, small changes in the density of large microplanktonic cells usually have a stronger effect on biomass (or chlorophyll, see Chisholm, 1992), thus supporting the relevance of the precise analysis of the size structure of phytoplankton in the study of seasonal, successional or productive cycles in the Antarctic waters and the ocean in general.

Acknowledgements

This study was financed by the Spanish CICYT project ANT94-1010. We would like to thank Marta Estrada and an anonimas referee for comments on a previous version of this manuscript. We thank the crew of the B.I.O. *Hespéricels* and all our colleagues during the FRUELA95 cruise for their help and cooperation.

References

Anadón, R., Estrada, M., 2002. The FRUELA Cruises. A carbon flux study in productive areas of the Antartic Peninsula (December 1995–February 1996). Deep-Sea Research II 49, 567–583.

Bianchi, F., Bodrin, A., Cioce, F., Dieckmann, G., Kuosa, H., Larsson, A.M., Nöthig, E.M., Sehlstedt, P.I., Socal, G., Syvertsen, E.E., 1992. Phytoplankton distribution in relation to sea ice, hydrography and nutrients in the northwestern Weddell Sea in early spring 1998 during EPOS. Polar Biology 12, 225–235.

Bienfang, P.K., Szyper, J.P., 1981. Phytoplankton dynamics in the subtropical Pacific Ocean of Hawaii. Deep-Sea Research 28, 981–1000.

Blanco, J.M., Echevarría, F., García, C.M., 1994. Dealing with size-spectra: some conceptual and mathematical problems. In: Rodríguez, J., Li, W.K.W. (Eds.), The Size Structure and Metabolism of the Pelagic Ecosystem. Scientia Marina 58, 17–29.

Chisholm, S.W., 1992. Phytoplankton size. In: Falkowski, P.G., Woodhead, A.D. (Eds.), Primary Productivity and Biochemical Cycles in the Sea. Plenum Press, New York, pp. 213–237.

Chisholm, S.W., Morel, F.M.M., 1991. Preface to "What controls phytoplankton production in nutrient-rich areas of the open sea?" Limnology and Oceanography, 36.

Cullen, J.J., 1991. Hypotheses to explain high-nutrient conditions in the open sea. Limnology and Oceanography 36 (8), 1578–1599.

Davidson, A.T., Marchant, H.L., 1992. Protist abundance and carbon concentration during a phaeocystis-dominated bloom at an Antarctic coastal site. Polar Biology 12, 387–395.

Echevarría, F., Rodríguez, J., 1994. The size structure of plankton during a deep bloom in a stratified reservoir. Hydrobiologia 284, 113–124.

El-Sayed, S.Z., 1971. Observations on phytoplankton bloom in the Weddel Sea. In: Llano, G.A.I., Wallen, E. (Eds.), Biology of Antarctic Seas (Ant Res Ser IV), Vol. 17. American Geophysical Union, Washington, pp. 301–312.

Estrada, M., Delgado, M., 1990. Summer phytoplankton distributions in the Weddell Sea. Polar Biology 10, 441–449.

Figueroa, F.L., 2002. Bio-optical characteristics of Gerlache and Bransfield Strait waters during an Antarctic summer cruise. Deep-Sea Research II 49, 675–691.

Fryxell, G.A., Kendrick, G.A., 1988. Austral Spring microalgae across the Weddel Sea ice edge: spatial relationships found along a northward transect during AMERIEZ 83. Deep-Sea Research 35, 1–20.

García, M.A., Castro, C.G., Ríos, A.F., Doval, M.D., Rosón, G., Gamis, D., López, O., 2002. Water masses and distribution of physico-chemical properties in the Western Bransfield and Gerlache Strain during austral summer 1995–96. Deep-Sea Research II 49, 585–602.

Helbling, E.W., Villafañe, V., Holm-Hansen, O., 1991. Effect of iron on productivity and size distribution of Antarctic phytoplankton. Limnology and Oceanography 36, 1879–1885.

Heywood, R.B., Whitaker, T.M., 1984. The Antarctic marine flora. In: Laws, R.M. (Ed.), Antarctic Ecology,, Vol. 2. Academic Press, London, pp. 373–419.

Holm-Hansen, O., Mitchell, B.G., 1991. Spatial and temporal distribution of phytoplankton and primary production in the western Bransfield Strait region. Deep-Sea Research II 38, 961–980.

Holm-Hansen, O., Mitchell, B.G., Hewes, C.D., Karl, D.M., 1989. Phytoplankton blooms in the vicinity of palmer station, Antarctica. Polar Biology 10, 49–57.

Jimenez-Gomez, 1995. Estructura de tamaños y dinámica del ultraplankton en el Ecosistema pelágico. Tesis Doctoral, Universidad de Málaga, 172pp.

Karl, D.M., Holm-Hansen, O., Taylor, G.T., Tien, G., Bird, D.F., 1991. Microbial biomass and productivity in the western Bransfield Strait, Antarctica during the 1986–87 austral summer. Deep-Sea Research II 38, 1029–1056.

Kopczynska, 1992. Dominance of microflagellates over diatoms in the Antarctic areas of deep vertical mixing and krill concentrations. Journal of Plankton Research 14, 1031–1054.

Lancelot, C., Mathot, S., Veth, C., de Baar, H., 1993. Factors controlling phytoplankton ice-edge blooms in the marginal ice-zone of the northwestern Weddel Sea during sea ice retreat 1988: field observations and mathematical modelling. Polar Biology 13, 377–387.

Laubscher, R.K., Perissinotto, R., McQuaid, C.D., 1993. Phytoplankton production and biomass at frontal zones in the Atlantic sector of the Southern Ocean. Polar Biology 13, 471–481.

Legendre, L., Le Fèvre, J., 1989. Hydrodynamical singularities as controls of recycled versus export production in oceans. In: Berger, W.H., Smetacek, V.S., Weter, G. (Eds.), Productivity of the Ocean. Present and Past. Wiley, Dahlem, pp. 49–63.

Li, W.K.W., 1994. Phytoplankton biomass and chlorophyll concentration across the North Atlantic. In: Rodríguez, J. Li, W.K.W. (Eds.), The Size Structure and Metabolism of the Pelagic Ecosystem. Scientia Marina 58, 67–79.

Margalef, R., 1978. Life-forms of phytoplankton as survival alternatives in an unstable environment. Oceanologica Acta 1, 493–509.

Mitchell, B.G., Holm-Hansen, O., 1991. Bio-optical properties of Antarctic Peninsula waters: differentiation from temperate ocean models. Deep-Sea Research II 38, 1009–1028.

Moline, M.A., Prezelin, B.B., 1996. Long-term monitoring and analyses of physical factors regulating variability in coastal antarctic phytoplankton biomass, in-situ productivity and taxonomic composition over subseasonal, seasonal and interannual time scales. Marine Ecology Progress Series 145, 143–160.

Mura, M.P., Satta, M.P., Agusti, S., 1995. Water-mass influence of summer Antarctic phytoplankton biomass and community structure. Polar Biology 15, 15–20.

Palmisano, A.C., SooHoo, J.B., SooHoo, S., Kottmeier, S.T., Craft, L.L., Sullivan, C.W., 1986. Photoadaptation in *Phaeocystis poucetti* advected beneath annual sea ice in McMurdo Sound, Antarctica. Journal of Plankton Research 8, 891–906.

Putt, M., Micelli, G., Stoecker, D.K., 1994. Association of bacteria with *Phaeocystis* sp. in McMurdo Sound, Antarctica. Marine Ecology Progress Series 195, 179–189.

Rodriguez, V., Guerrero, F., 1994. Chlorophyll *a* of size-fractionated summer phytoplankton blooms at a coastal station in Málaga Bay, Alboran Sea. Estuarine. Coastal and Shelf Science 39, 413–419.

Rodríguez, J., Li, W.K.W. (Eds.), 1994. The size structure and metabolism of the pelagic ecosystem. Scientia Marina 58(1–2) 167.

Rodriguez, J., Blanco, J.M., Jimenez-Gomez, F., Echevarría, F., Gil, J., Rodríguez, V., Ruiz, J., Bautista, B., Guerrero, F., 1998. Patterns in the size structure of the phytoplankton community in the deep fluorescence maximum of the Alboran Sea (Southwestern Mediterranean). Deep-Sea Research I 45, 1577–1593.

Ruiz, J., García, C.M., Rodriguez, J., 1996. Sedimentation loss of phytoplankton cells from the mixed layer: effects of turbulence levels. Journal of Plankton Research 18, 1727–1734.

Savidge, G., Harbour, D., Gilpin, L.C., Boyd, P.W., 1995. Phytoplankton distribution and production in the Bellingshausen Sea, Austral Spring 1992. Deep-Sea Research II 42, 1201–1224.

Schloss, I., Estrada, M., 1994. Phytoplankton composition in the Weddell-Scotia Confluence area during austral spring in relation to hydrography. Polar Biology 14, 77–90.

Smetacek, V., Scharek, R., Nöthig, E.M., 1990. Seasonal and regional variation in the pelagial and its relationship to the life history cycle of krill. In: Kerry, K.R., Hempel, G. (Eds.), Antarctic Ecosystems. Ecological Change and Conservation. Springer, Berlin, pp. 103–114.

Smith, W.O., Nelson, D.M., 1985. Phytoplankton bloom produced by a receding ice-edge in the Ross Sea: spatial coherence with the density field. Science 227, 163–165.

Socal, G., Nöthig, E.M., Bianchi, F., Boldrin, A., Mathot, S., Rabitti, S., 1997. Phytoplankton and particulate matter at

the Weddell/Scotia Conflunce (47°W) in summer 1989, as a final step of a temporal succession (EPOS project). Polar Biology 18, 1–9.

Stoecker, D.K., Putt, M., Moisan, T., 1995. Nano- and microplankton dynamics during the spring *Phaeocystis* sp. bloom in McMurdo Sound, Antarctica. Journal of the Marine Biological Association of the United Kingdom 75, 815–832.

Treguer, P., Jacques, G., 1992. Dynamics of nutrients and phytoplankton, and fluxes of carbon, nitrogen and silicon in the Antarctic Ocean. Polar Biology 12, 149–162.

Varela, M., Fernández, E., Serret, P., 2002. Size-fractionated phytoplankton biomass and primary production in the Gerlache and South Bransfield Straits (Antarctic Peninsula) in the Austral summer 1995–1996. Deep-Sea Research II 49, 749–768.